Carbohydrate Polymers 114 (2014) 206–212

Contents lists available at ScienceDirect

Carbohydrate Polymers

journal homepage: www.elsevier.com/locate/carbpol

Changes of structure and property of alkali soluble hydroxyethyl celluloses (HECs) and their regenerated films with the molar substitution

Faxue Li[a,b,*], Wencong Wang[a,b], Xueli Wang[c], Jianyong Yu[c]

[a] The Key Lab of Textile Science and Technology Ministry of Education, Shanghai 201620, China
[b] College of Textiles, Donghua University, Shanghai 201620, China
[c] Modern Textile Institute, Donghua University, Shanghai 200051, China

ARTICLE INFO

Article history:
Received 2 July 2014
Received in revised form 28 July 2014
Accepted 8 August 2014
Available online 18 August 2014

Keywords:
Hydroxyethyl celluloses (HECs)
Molar substitution (MS)
Structure
Properties

ABSTRACT

Hydroxyethyl celluloses (HECs) with low molar substitutions (MS) were prepared by reaction of alkali cellulose with ethylene oxide (EO) in a heterogeneous process. NMR, FTIR, WAXD, TG, solubility and tensile tests were adopted to investigate the changes of structures and properties of HECs with their MS values. NMR results showed that the hydroxyethyl groups were introduced into the cellulose chains as expected, causing the destruction in ordered structure and a loss in crystallinity. Crystal transformation from cellulose I of raw cellulose to cellulose II of HECs was proved by different methods. The crystalline structure of HEC seriously deteriorated with the rising MS value, accompanying lower thermal stability and improvements on its solubility in 8 wt% NaOH solvent and moisture related properties such as water retention. These different properties depending on the MS values endowed HECs with various potential applications in the form of regenerated cellulose fibers or other absorbent materials.

1. Introduction

As the most abundant renewable resource, cellulose is a promising material and has attracted much attention due to the great significance for sustainable development (Bledzki & Gassan, 1999; Chandra & Rustgi, 1998; Schurz, 1999). However, cellulose still has not reached its potential application in many areas because it is difficult to process in general solvents or in the melting state on account of its strong inter- and intra-molecular hydrogen bonding. Based on its unique structure and reactivity, chemical modification continues to play a dominant role in improving the overall utilization of the biomacromolecules (Heinze, 1998; Heinze, Liebert, Klüfers, & Meister, 1999; Klemm, Heinze, Philipp, & Wagenknecht, 1997).

Traditionally, viscose technology is still the most widely used route to manufacture regenerated cellulose fibers, which is accompanied with hazardous byproducts such as CS_2, H_2S and heavy metals (Philipp, 1993). A limited number of novel solvents for cellulose were reported in the past decades such as N-methylmorpholine-N-oxide (NMMO) (Fink, Weigel, Purz, & Ganster, 2001), ionic liquids (IL) (El Seoud, Koschella, Fidale, Dorn, & Heinze, 2007; Vitz, Erdmenger, Haensch, & Schubert, 2009; Zhu et al., 2006), NH_3/NH_4SCN (Hudson & Cuculo, 1980), N, N-dimethylacetamide (DMAc)/LiCl (Williamson & McCormick, 1998), $ZnCl_2$ aqueous solution (Xu & Chen, 1994), dimethyl sulfoxide (DMSO)/tetrabutylammonium fluoride (Köhler & Heinze, 2007). Most of these solvents are limited on a pilot-scale except for NMMO, which has been commercially used to produce regenerated cellulose fibers called Lyocell. Unfortunately, NMMO still has the problems like high temperature to dissolve, high cost, degradation of cellulose and the solvent itself in production (Liu et al., 2011). There is a growing urgency to develop a novel nonpolluting process to utilize cellulose or its derivatives for fiber preparation in the cellulose industries for the purpose of environmental conservation.

Hydroxyethyl cellulose (HEC), one of the most important cellulose derivatives, is commercially produced by reaction of alkali cellulose with ethylene oxide (EO) in a heterogeneous process. HEC can be employed in extensive utilization because of its wonderful properties and chemical composition with a large amount of relatively easily accessible hydroxyl units that can be bonded with a number of functional groups (Erkselius & Karlsson, 2005; Liedermann & Lapcık, 2000; Sun, Sun, Wei, Liu, & Zhang, 2007). According to the different etherification degrees of HEC, it exhibits

* Corresponding author at: The Key Lab of Textile Science and Technology Ministry of Education, Shanghai 201620, China. Tel.: +86 21 6779 2803; fax: +86 21 6779 2627.
E-mail address: fxlee@dhu.edu.cn (F. Li).

http://dx.doi.org/10.1016/j.carbpol.2014.08.015
0144-8617/

different solubility and is generally divided into water-soluble and alkali-soluble products. Nowadays, water-soluble HEC has been extensively used as stabilizer in food and cosmetic products, binder in tablets, thickener in latex paints, water-binder in welding rods or glazes of ceramics and in building materials applications in industry (Adden, Müller, Brinkmalm, Ehrler, & Mischnick, 2006; Guo, Skinner, Harcum, & Barnum, 1998). However, the application of alkali-soluble HEC with low substitution is limited. With the good film- and fiber-forming properties, the correlative technology on alkali-soluble HEC is expected to substitute the traditional viscose route due to its nonpolluting, cheaper and shorter flow of production.

In the previous studies of our laboratory (Wang et al., 2013), regenerated HEC fibers with good tensile properties were successfully prepared by dispersing the alkali-soluble HEC into novel NaOH/urea/thiourea solvent, indicative of great potential in substituting traditional viscose technology. However, the addition of urea and thiourea as the assistant solvent would definitely bring extra loads in their recycling or disposal in the approaching industrial production. So there is no better if only NaOH aqueous solution is regarded as the solvent for dissolving the cellulose due to the cheapness and abundant sources of NaOH. But as is known to all, NaOH aqueous solution merely swells the cellulose or partially dissolves the cellulose with low degree of polymerization due to the strong inter- and intra-molecular hydrogen bonding. Hence, it is not unnecessary to weaken hydrogen bonding of cellulose by enlarging the gap between the macromolecular chains. Contributed to the formation of small side chains in cellulose ring during the etherification reaction, HEC is apt to have larger gap between the macromolecular chains and corresponding weaker inter- and intramolecular hydrogen bonding, which is beneficial for NaOH solution to dissolve the material.

In this paper, we focused on the preparation of alkali-soluble HECs with various MS values during the gas–solid etherification reaction, followed by exploring the dissolution of the as-prepared HECs in NaOH aqueous solution with a simple and environment-friendly method. The changes of structures and properties of HECs and resultant regenerated films with the MS values were intensively investigated with a couple of techniques, aiming at providing a more fundamental support for the following process of wet spinning.

2. Experimental

2.1. Materials

Cotton linters with degree of polymerization of 1000 were purchased from Xiangtai Corporation (Hubei Province, China). EO, NaOH and glacial acetic acid supplied by Enterprise group chemical reagent Co., LTD were analytical reagent and used without further purification. Reactor and disintegrator were custom-made.

2.2. Preparation of HECs

2.2.1. Synthesis of HECs

HEC was synthesized in a heterogeneous process as described in the previous report (Wang et al., 2013). Cellulose powders predried in vacuum were immersed in 21 wt% NaOH aqueous solution with vigorous stirring at ambient temperature. Alkaline cellulose gained through squeezing was transferred into a homemade 2 L stainless steel autoclave equipped with a mechanical stirrer. A certain amount of liquid EO was added into the vacuum autoclave simultaneously. The mixtures were stirred at 40 °C for 100 min to make the gasified EO fully react with alkaline cellulose powders. The etherification reaction was terminated as the pressure inside the autoclave nearly returned to the initial value. The as-products were neutralized with acetic acid, repeatedly rinsed with distilled water, and then dried under vacuum. Samples prepared by changing the feeding mass ratio of EO to raw cellulose from 0.00, 0.05, 0.10, 0.20, 0.30, 0.40 to 0.50 were signed as a, b, c, d, e, f and g, respectively.

2.2.2. Preparation of HEC/NaOH solution

HEC/NaOH solution with concentration of 5 wt% was prepared by dispersing a certain amount of dried HEC powders into 8 wt% NaOH aqueous solution pre-cooled at −6 °C, and then the mixtures were stirred vigorously at −5 to 0 °C for 2 h to get transparent solution.

2.2.3. Preparation of HEC films

After filtration, the 5 wt% HEC solutions owning various MS values were subjected to centrifugation at 5000 rpm for 10 min at ambient temperature to eliminate bubbles. The transparent solutions were immediately cast on glass slides, and the thickness of wet film was controlled to be around 0.5 mm. The sheets were immersed into coagulation bath composed of 10 wt% acetic acid solution for 30 min. The resultant HEC films were subsequently washed by distilled water until the pH value reached 7, followed by drying them at 20 °C under vacuum for 24 h.

2.3. Characterizations

2.3.1. Nuclear magnetic resonance (NMR) measurements

The HECs could be dissolved in $CDCl_3$ through acetylated reaction with acetic acid (Tezuka, Imai, Oshima, & Chiba, 1989). ^{1}H-NMR measurements on these acetylated HEC solutions with different MS values were performed on a Bruker Avance 400 Nuclear Magnetic Resonance Spectrometer in the proton noise-decoupling mode with a standard 5 mm probe at ambient temperature, and the sample concentration was about 3.5 wt%.

Solid state ^{13}C-NMR spectra of raw cellulose and HECs were recorded on Avance 400 spectrometer (Bruker Inc., Switzerland) with a cross polarization/magic angle spinning (CP/MAS) unit at ambient temperature.

2.3.2. Fourier transformed infrared spectroscopy (FTIR) measurements

FTIR spectra of raw cellulose and HECs were recorded with a Nicolet NEXUS-670 Fourier transform infrared spectrometer. The samples dried by infrared lamp were cut into fine powders and mixed with KBr, and then the mixtures were pressed to give a slice for FTIR measurements.

2.3.3. Wide angle X-ray diffraction (WAXD) measurements

X-ray diffraction technique was employed to investigate the crystalline structures of HECs at room temperature. The measurements were conducted with a Rigaku D/max 2550VB/PC diffraction instrument. The power of the generator is 40 kV and 200 mA with a Nickel-filtered Cu K_α radiation (λ = 0.154 nm). The X-ray diffraction profiles were recorded at the 2θ range of 6–40° at a scanning speed of 8°/min. The crystallinities of samples were calculated according to the peak separation. Individual crystal reflection peak and amorphous background were extracted by the curve-fitting process of the diffraction intensity profile with the software MDI Jade 5. The crystallinity was estimated as the ratio of the total crystal peak intensity to the total diffraction intensity.

2.3.4. Thermal gravimetric analysis (TGA)

Thermal stability of raw cellulose and HECs was determined with a Netzsch TG 209F1 thermo-gravimetric analyzer. The

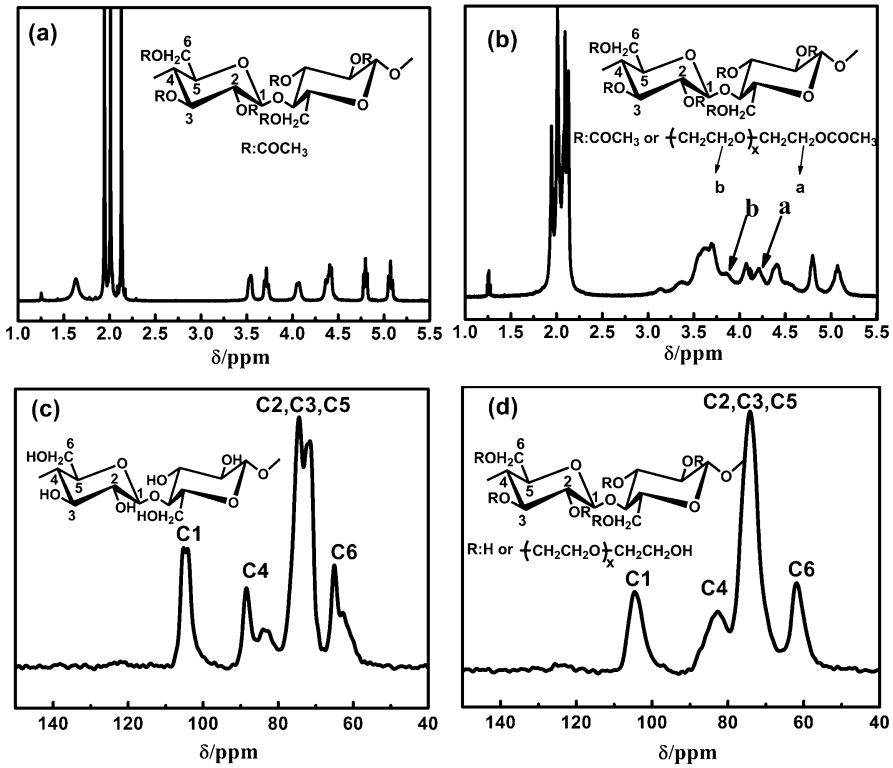

Fig. 1. The ^{1}H-NMR spectra of acetylated cellulose (a) and HEC (b) in $CDCl_3$ at 25 °C, and solid-state ^{13}C-NMR curves of raw cellulose (c) and HEC (d).

specimens were tested in N_2 atmosphere and heated up to 600 °C at a heating rate of 10 °C/min.

2.3.5. Solubility determination of HEC samples

A certain mass (M_1) of HEC solutions with concentration of 5 wt% was selected to check the solubility of HEC in 8 wt% NaOH solution. Undissolved residues in the NaOH solution were collected by filtration on a glass filter, and then rinsed successively with 8% NaOH solution, water, dilute acetic acid and acetone at room temperature. The remains were weighed as M_0 after drying in vacuum. The solubility values (S_a) of these samples were expressed as the percentage of the total amount of HECs that passed through the filter.

$$S_a(\%) = [(M_1 \times 5\% - M_0)/(M_1 \times 5\%)] \times 100 \quad (1)$$

2.3.6. Evaluation of water retention value (WRV)

HEC film was soaked into distilled water for 2 h at ambient temperature, and then centrifuged at a relative centrifugal force (RCF) of 1000 g for 20 min, after which the weight of the wet film was determined as W_0. Subsequently, the sample was dried at 105 °C until its weight kept constant, and reweighed to be W_1. The water retention value (*WRV*) was calculated from Eq. (2).

$$\mathrm{WRV}(\%) = (W_0 - W_1)/W_1 \times 100 \quad (2)$$

2.3.7. Tensile test of HEC films

The tensile properties of HEC films with different MS values were measured on a universal tensile tester (HD026N+, Nantong Hongda experiment instruments, China) according to the standard method ISO 527-2, 1993(E). The width of the specimen was 10 mm and the length was 40 mm. The film thickness was measured with fabric thickness meter (YG141D, Changzhou Textile Instrument Co., Ltd, China) under the presser foot area of 100 mm^2 and pressure weight of 50 cN. The films were preconditioned for 1 day so that they reached the standard atmospheric equilibrium of 65% relative humidity (RH) at 20 °C. A gauge length of 30 mm was applied and the tensile speed was 10 mm/min. The tensile results were determined from the average value of five-time tests.

3. Results and discussion

3.1. Structural development of HEC with the MS value

Fig. 1a and b presents the ^{1}H-NMR spectra of acetylated cellulose and HEC, respectively. The three peaks from 1.90 to 2.10 ppm were assigned to protons of CH_3—CO—O— group, which was produced by acetylated reaction with three hydroxyls of cellulose, while the broad peaks between 3.50 and 5.10 ppm were attributed to the signals of six protons in the anhydroglucose unit (AGU). Furthermore, it can be found that some new peaks emerged in the spectrum of acetylated HEC as shown in Fig. 1b. The peak at 4.20 ppm was contributed to the protons of O—CH_2—CH_2— close to —CH_3, whereas the small peak at 3.71 ppm was assigned to protons of the other O—CH_2—CH_2- groups. The three peaks from 1.90 to 2.10 ppm were split into four peaks since some of hydroxyls attached to the AGU were replaced by the hydroxyethyl groups. These new peaks verified that the hydroxyethyl groups were introduced into the cellulose chains as expected. In addition, the MS values of HECs could be estimated from the peak area of 4.20 ppm and 3.71 ppm via the previous method reported by Heinze (Heinze & Liebert, 2001). For the b–g samples, their corresponding MS values were determined to be 0.09, 0.17, 0.30, 0.48, 0.65 and 0.84 as presented in Table 2, respectively.

Fig. 1c and d shows the solid state ^{13}C-NMR spectra of raw cellulose and HEC. It is noted that four main peaks in the spectrum of HEC appear at 104.5, 82.8, 74.1 and 61.8 ppm, assigned to C1, C4, (C2,C3,C5) and C6. Compared with raw cellulose, C4 and C6 signals of the HEC shifted to higher magnetic field as a single peak, corresponding to the shoulder peaks of cellulose attributing to C4 and C6 signals located in amorphous region, suggesting that the partial destruction of ordered structure and the loss of

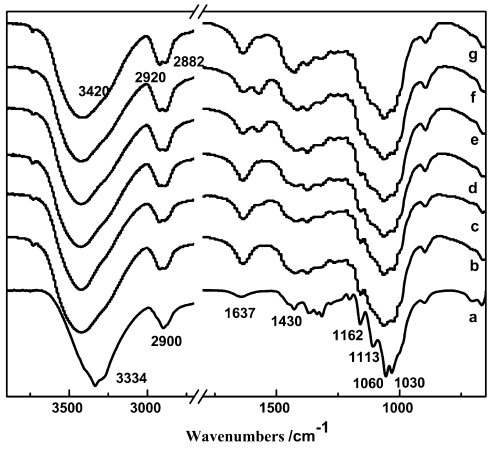

Fig. 2. FTIR spectra of raw cellulose (a) and HECs with different MS values (b–g).

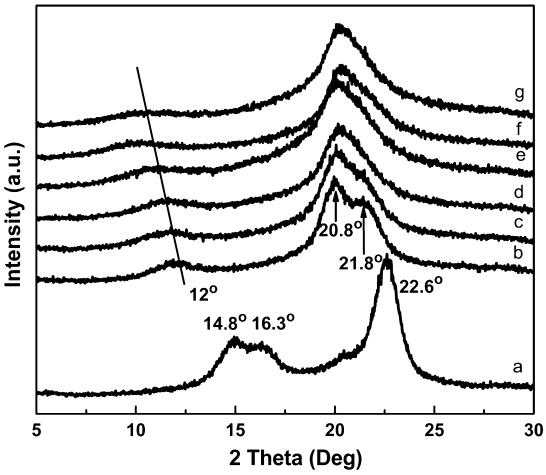

Fig. 3. X-ray diffraction patterns of raw cellulose (a) and HECs (b–g).

crystallinity occurred due to the substituent groups (Clark, Fowler, & Stephenson, 1983). Meanwhile, the change in C6 signals also verified the transformation of the C6—OH group from the "*t*-*g*" conformation for the crystalline region of cellulose I to a "*g*-*t*" conformation of cellulose II (Isogai, Usuda, Kato, Uryu, & Atalla, 1989). It was hard to obtain the information of C2, C3 and C5 from the Fig. 1c and d, which was perhaps due to the overlap of broad peaks at 74.1 ppm.

Fig. 2 shows the FTIR spectra of cellulose and HECs with various MS values. A broad absorption band around 3720–3000 cm^{-1} for these samples was ascribable to the stretching vibration of —OH group. For comparison with cellulose, the absorption peak of the band in the spectra of HECs was shifted distinctly from 3334 cm^{-1} to higher wave number of 3420 cm^{-1} as a result of the decrease in intra- and inter-molecular bonds caused by hydroxyethylation. The characteristic peaks from 2800 to 3000 cm^{-1} were assigned to the stretching vibration of —CH_2— group, among which the band changed from 2900 cm^{-1} for cellulose to around 2920 cm^{-1} for the hydroxyethylated samples. New small shoulders emerged in the spectra of HECs and their position shifted to lower wave numbers from 2891 cm^{-1} to 2882 cm^{-1} with the increasing MS value, indicative of the presence of —CH_2— groups. The 1430 cm^{-1} band assigned as symmetric —CH_2 bending vibration was transferred to around 1418 cm^{-1} accompanied with a considerable decrease in absorbance intensity after hydroxyethylation, manifesting the conformation of CH_2OH at C6 was converted from the "*t*-*g*" to the "*g*-*t*" form. The characteristic band at 1162 cm^{-1} representing the stretching vibration of C—O—C at β-glucosidic linkage was sharp for cellulose but vanished gradually as the MS value increased, while the peak at 1032 cm^{-1} assigned to stretching vibration of C—O at C6 was shifted to 1019 cm^{-1} after introducing the hydroxyethyl groups, which may be affected by the variation of hydrogen bonding during the crystal form transformation (Heinze et al., 1999).

Fig. 3 illustrates the X-ray diffraction patterns of raw cellulose and HECs. The raw cellulose displayed the cellulose I structure with typical diffraction peaks at $2\theta = 14.8°$ for $(\bar{1}\,1\,0)$, 16.3° for (1 1 0) and 22.6° for (0 2 0), while HECs possessed the characteristic cellulose II structure at 12.1° for $(\bar{1}\,1\,0)$, 20.8° for (1 1 0) and 21.8° for (0 2 0) (Langan, Sukumar, Nishiyama, & Chanzy, 2005), further conforming that the transition of cellulose I into cellulose II occurred during etherification process. Meanwhile, the peaks of plane (0 2 0) gradually disappeared, but in fact they were merged into the peaks of plane (1 1 0) whose position almost maintained fixed in the spectra of HECs, because the most abundant -OH groups existed inside the plane (1 1 0) where the etherification reaction mainly took place. The peak of $(\bar{1}\,1\,0)$ was shifted to a lower angle as a result of the increasing inter-planar distance of plane $(\bar{1}\,1\,0)$ ($d(\bar{1}\,1\,0)$) due to the introduced substituent groups.

Crystallinity variation of HECs with the various MS values is listed in Table 2. As expected, HECs exhibited a lower crystallinity than raw cellulose due to the introduction of side chains during etherification process, which weakened the arranging regularity of cellulose macromolecules. Furthermore, the crystallinities of HECs decreased monotonously with the rising MS value. The possible reason was attributed to the different reaction rate of the hydroxyls at different position of the cellulose ring. It was reported that the order of relative reaction rate of hydroxyls in the ring was C2:C3:C6:C_{HE} = 3:1:10:20 (C_{HE} means the carbons of hydroxyethyl groups at the side chain) (Stratta, 1963), leading to the random distribution and various chain lengths of the substituents embedding into the cellulose bone chains. Therefore, structural regularity of cellulose would be breached and the crystallinities of HECs were lowered. The more EO consumed in the etherification reactions, the more damage to cellulose crystalline structure.

3.2. Thermal properties of HECs

Thermal stability of cellulose and its derivatives is the important performance that restricts their application due to the occurrence of rapid chemical decomposition at high temperature, and the characteristics of substituents bonding with cellulose chains have great influences on their thermal stability (Kissinger, 1957). Fig. 4 plots the TG and DTG curves of cellulose and HECs at a heating rate of 10 °C/min under nitrogen atmosphere. Obviously, the TG curves of HECs shifted to left side with their increasing MS values, suggesting that the introduction of substituents into the cellulose chains deteriorated their thermal stabilities. Furthermore, each curve showed the typical characteristics of three distinct zones. The initial weight loss in the first stage was attributed to the evaporation of residual absorbed water, and then followed by the main depolymerization and decompositon of the polymers in the second stage. The curves showed a sharp weight loss at the range of 260–380 °C due to the formation of volatiles like CO or CH_4. In the last stage, there was a very slow approach to constant weight accompanying the reactions of pyrolysis and carbonization.

Table 1 lists the parameters such as initial weight loss, onset decomposition temperature (T_d), the temperature at the maximum degradation rate (T_{dm}) and residual mass at 600 °C for various samples according to these curves. The initial weight loss of HECs increased as their MS values went up, indicating that they would

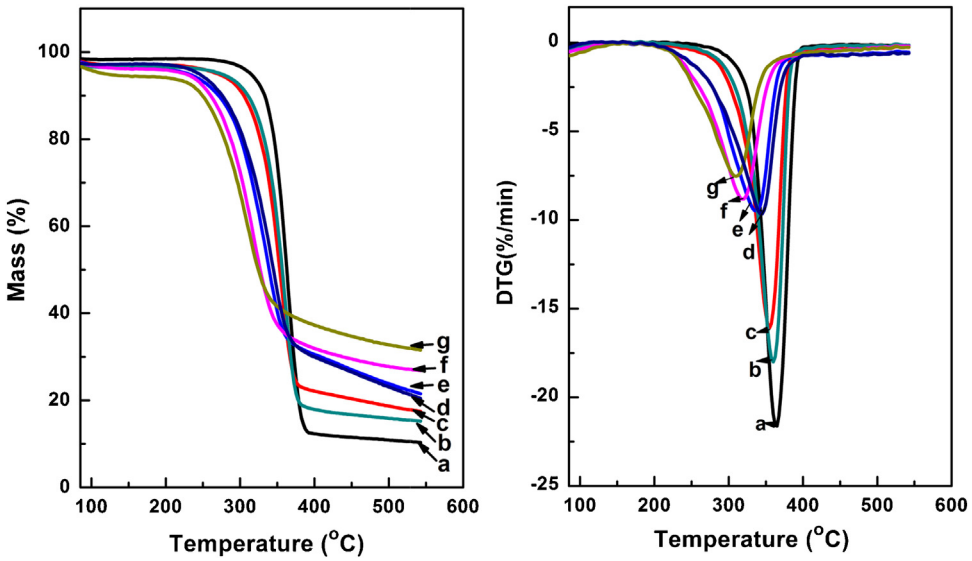

Fig. 4. TG (left) and DTG (right) curves of raw cellulose (a) and HECs (b–g).

possess much more excellent moisture absorbance because more hydrophilic hydroxyethyl groups were introduced into cellulose chains. In addition, the T_d and T_{dm} for HECs slid gradually with the increasing MS value, while the residual mass was rising, which was in accordance with the results in pervious literature (Li, Huang, & Bai, 1999) that the hydroxyethyl groups lowered significantly the pyrolytic temperature, retarded polymeric carbonization and increased pyrolysis residues. The samples would become less stable under thermal treatment as the MS value increased, corresponding to their crystallinity changes mentioned above. Thus, conclusions were drawn that the introduction of hydroxyethyl groups resulted in the increase of amorphous regions and partial destroy of hydrogen bonds, which made these polymers more vulnerable under thermal suffering.

3.3. Solubility and moisture related properties of HECs

Generally, it is hard for cellulose to be dissolved in alkali solvent, but the solubility is evidently improved for etherified cellulose due to the reduced density of hydrogen bonds, partial destruction of crystalline structure and introduced hydrophilic substituents during etherification. HEC with low MS value which is readily soluble in alkali solvent and maintains stable in water presents great potentials in substituting the traditional viscose technology. However, the amount of hydroxyethyl groups embedded into cellulose chains has significant impacts on the solubility and fiber formation. Thus, it is of great importance to optimize the MS value of HEC used for wet spinning.

Table 2 shows the solubilities (S_a) of HECs with different MS values in 8 wt% NaOH aqueous solution. It could be seen that the S_a value of HEC in the dilute alkali solution increased dramatically after etherification especially when the MS value was above 0.17, where the solubility reached around 98%. As the MS value further increased, the solubility seemed to level off.

Water retention, as an indicator to investigate the interaction between liquid or gaseous water and HEC, has a significant influence on the processing and application of HEC. As seen in Table 2, the WRV increased dramatically from 86% for cellulose to 326% for HEC with a MS value of 0.84. It was obvious that the water retention of HEC was closely associated with the MS value, because water molecules tended to have increasing affinity with HEC macromolecules as the amount of hydroxyethyl groups introduced was elevated. Besides, based on the results from X-ray diffraction, more amorphous regions caused by etherification reaction were beneficial to holding more water. These alkali soluble HECs possessed excellent water retention especially when the MS value exceeded 0.30, showing great potentials in medical application as healthy and green absorbent materials. However, it was ought to point out the samples with MS values higher than 0.30 were inclined to dramatically swell in water bath as a result of strong attraction to water, and were unsuitable for continuous wet spinning.

3.4. Tensile properties of HEC films

Table 3 summarizes the parameters of tensile property of HEC films with various MS values. It could be found that the MS values of HEC films had great influences on their tensile properties. The HEC-b film had the highest tensile strength although the concentration of the polymer solution was slightly lower than any others due to the partial dissolution in 8 wt% NaOH solution as

Table 1
Characteristic parameters of thermal decomposition of various samples.

Samples	Cellulose-a	HEC-b	HEC-c	HEC-d	HEC-e	HEC-f	HEC-g
Initial mass loss (wt%)[a]	1.66	2.80	2.86	3.48	3.55	3.79	5.41
T_d (°C)[b]	341.6	334.2	326.7	298.4	292.8	276.1	267.0
T_{dm} (°C)[c]	363.9	359.8	354.9	343.8	336.7	318.7	309.5
Residual mass (wt%)	9.63	14.65	16.26	17.41	18.7	25.81	30.41

[a] The mass loss of samples during the first 100 °C.
[b] The onset temperature of decomposition.
[c] The temperature corresponding to the maximum degradation rate.

Table 2
Physical properties of raw cellulose and HECs with different MS values.

	Cellulose-a	HEC-b	HEC-c	HEC-d	HEC-e	HEC-f	HEC-g
Mass ratio of EO to cellulose	0	0.05	0.10	0.20	0.30	0.40	0.50
MS value	0	0.09	0.17	0.30	0.48	0.65	0.84
Crystallinity (%)	68.4	57.7	50.7	46.9	41.9	40.0	37.4
WRV (%)	86	146	155	168	259	282	326
Solubility in 8wt% NaOH (%)	1.49	85.1	97.3	97.9	98.2	98.3	98.5

Table 3
Tensile properties of HEC films with different MS values.

HEC films	HEC-b	HEC-c	HEC-d	HEC-e	HEC-f	HEC-g
Thickness (mm)	0.09	0.10	0.11	0.13	0.10	0.11
Tensile strength (Mpa)	72.5	47.5	41.2	21.8	20.9	15.8
Elongation at break (%)	7.80	7.85	8.40	8.65	8.75	11.20

shown in Table 2. With the rising of MS value, the tensile strengths of HEC films fell, whereas the elongation at break went up. The higher MS value the HEC film had, which meant the more hydroxyethyl groups were introduced into the cellulose chains, the less regular crystalline structure the HEC would have. The distances between macromolecular chains were enlarged due to the growing length of side chains as well as the steric hindrance of substituent groups which had been confirmed by WAXD investigations. The hydrogen bonding between macromolecular chains was greatly weakened by the excessive hydroxyethyl groups which reacted with the hydroxyl groups at C2, C3 and C6 positions and acted as a wedge among these chains. Therefore, it was much easier for molecular chains of HEC films with high MS values to slide over one another as they were applied to the load. Meanwhile, when the molecular chains with slipping of dislocation tended to be aligned parallel, it was still difficult for them to form physical bonds at new positions due to the weak interaction between molecular chains. Unfortunately, HEC samples with high MS values could not guarantee enough tensile strength, which was apt to limit their utilizations.

In general, HECs with the MS value of 0.17–0.30 are suitable for manufacturing the HEC regenerated fibers due to its good solubility in dilute NaOH solvent, moderated water retention and good tensile properties after regeneration. Meanwhile, the HECs with their MS values higher than 0.30 (lower than 1.0) are potential to be applied as the water absorbent materials which require high water retention but relatively low mechanical properties.

4. Conclusions

In this study, a series of alkali soluble HECs with low MS values were successfully prepared by the gas-solid reaction of EO with alkali-cellulose in a heterogeneous process. The MS values of the alkali-soluble HECs were calculated from ^{1}H-NMR, and the crystal form transition from cellulose I to cellulose II was verified by FTIR, ^{13}C-NMR and WAXD. Besides, it was confirmed that the crystallinities and thermal stabilities of HECs were decreased gradually with the rising MS value, while their solubility in 8 wt% NaOH solvent and moisture related properties such as water retention were boosted. On the basis of the results from solubility, water retention and tensile properties, it could be learned that HECs with the MS value of 0.17–0.30 were suitable for the subsequent research of wet spinning, while HECs with the MS value higher than 0.3 may be potential as water absorbing materials which require high water retention but relatively low mechanical properties. The HECs with low MS values must bring wide application prospect in the cellulose industry.

Acknowledgments

This work has been financially supported by the Fundamental Research Funds for the Central Universities, to which the authors express their gratitude.

References

Adden, R., Müller, R., Brinkmalm, G., Ehrler, R., & Mischnick, P. (2006). Comprehensive analysis of the substituent distribution in hydroxyethyl celluloses by quantitative MALDI-ToF-MS. *Macromolecular Bioscience*, *6*(6), 435–444.
Bledzki, A., & Gassan, J. (1999). Composites reinforced with cellulose based fibres. *Progress in Polymer Science*, *24*(2), 221–274.
Chandra, R., & Rustgi, R. (1998). Biodegradable polymers. *Progress in Polymer Science*, *23*(7), 1273–1335.
Clark, D., Fowler, A., & Stephenson, P. (1983). Application of modern analytical techniques to the investigation of cellulose nitrates. *Journal of Macromolecular Science-Reviews in Macromolecular Chemistry and Physics*, *23*(2), 217–246.
El Seoud, O. A., Koschella, A., Fidale, L. C., Dorn, S., & Heinze, T. (2007). Applications of ionic liquids in carbohydrate chemistry: A window of opportunities. *Biomacromolecules*, *8*(9), 2629–2647.
Erkselius, S., & Karlsson, O. J. (2005). Free radical degradation of hydroxyethyl cellulose. *Carbohydrate Polymers*, *62*(4), 344–356.
Fink, H. P., Weigel, P., Purz, H., & Ganster, J. (2001). Structure formation of regenerated cellulose materials from NMMO-solutions. *Progress in Polymer Science*, *26*(9), 1473–1524.
Guo, J., Skinner, G., Harcum, W., & Barnum, P. (1998). Pharmaceutical applications of naturally occurring water-soluble polymers. *Pharmaceutical Science & Technology Today*, *1*(6), 254–261.
Heinze, T. (1998). New ionic polymers by cellulose functionalization. *Macromolecular Chemistry and Physics*, *199*(11), 2341–2364.
Heinze, T., & Liebert, T. (2001). Unconventional methods in cellulose functionalization. *Progress in Polymer Science*, *26*(9), 1689–1762.
Heinze, T., Liebert, T., Klüfers, P., & Meister, F. (1999). Carboxymethylation of cellulose in unconventional media. *Cellulose*, *6*(2), 153–165.
Hudson, S. M., & Cuculo, J. (1980). The solubility of cellulose in liquid ammonia/salt solutions. *Journal of Polymer Science: Polymer Chemistry Edition*, *18*(12), 3469–3481.
Isogai, A., Usuda, M., Kato, T., Uryu, T., & Atalla, R. H. (1989). Solid-state CP/MAS carbon-13 NMR study of cellulose polymorphs. *Macromolecules*, *22*(7), 3168–3172.
Köhler, S., & Heinze, T. (2007). New solvents for cellulose: Dimethyl sulfoxide/ammonium fluorides. *Macromolecular Bioscience*, *7*(3), 307–314.
Kissinger, H. E. (1957). Reaction kinetics in differential thermal analysis. *Analytical Chemistry*, *29*(11), 1702–1706.
Klemm, D., Heinze, T., Philipp, B., & Wagenknecht, W. (1997). New approaches to advanced polymers by selective cellulose functionalization. *Acta Polymerica*, *48*(8), 277–297.
Langan, P., Sukumar, N., Nishiyama, Y., & Chanzy, H. (2005). Synchrotron X-ray structures of cellulose Iβ and regenerated cellulose II at ambient temperature and 100 K. *Cellulose*, *12*(6), 551–562.
Li, X., Huang, M., & Bai, H. (1999). Thermal decomposition of cellulose ethers. *Journal of Applied Polymer Science*, *73*(14), 2927–2936.
Liedermann, K., & Lapcık, L., Jr. (2000). Dielectric relaxation in hydroxyethyl cellulose. *Carbohydrate Polymers*, *42*(4), 369–374.
Liu, Z., Wang, H., Li, Z., Lu, X., Zhang, X., Zhang, S., et al. (2011). Characterization of the regenerated cellulose films in ionic liquids and rheological properties of the solutions. *Materials Chemistry and Physics*, *128*(1), 220–227.
Philipp, B. (1993). Organic solvents for cellulose as a biodegradable polymer and their applicability for cellulose spinning and derivatization. *Journal of Macromolecular Science, Part A: Pure and Applied Chemistry*, *30*(9–10), 703–714.
Schurz, J. (1999). A bright future for cellulose. *Progress in Polymer Science*, *24*(4), 481–483.
Stratta, J. J. (1963). A statistical analysis of the distribution of substituents for soluble and insoluble hydroxyethyl cellulose. *Tappi Journal*, *46*, 717–722.
Sun, W., Sun, D., Wei, Y., Liu, S., & Zhang, S. (2007). Oil-in-water emulsions stabilized by hydrophobically modified hydroxyethyl cellulose: Adsorption and thickening effect. *Journal of Colloid and Interface Science*, *311*(1), 228–236.
Tezuka, Y., Imai, K., Oshima, M., & Chiba, T. (1989). Determination of substituent distribution in cellulose ethers by means of a 13 C nuclear magnetic resonance study on their acetylated derivatives: 3 Hydroxyethylcellulose. *Polymer*, *30*(12), 2288–2291.

Vitz, J., Erdmenger, T., Haensch, C., & Schubert, U. S. (2009). Extended dissolution studies of cellulose in imidazolium based ionic liquids. *Green Chemistry*, *11*(3), 417–424.

Wang, W., Zhang, P., Zhang, S., Li, F., Yu, J., & Lin, J. (2013). Structure and properties of novel regenerated cellulose fibers prepared in NaOH complex solution. *Carbohydrate Polymers*, *98*(1), 1031–1038.

Williamson, S. L., & McCormick, C. L. (1998). Cellulose derivatives synthesized via isocyanate and activated ester pathways in homogeneous solutions of lithium chloride/N, N-dimethylacetamide. *Journal of Macromolecular Science—Pure and Applied Chemistry*, *35*(12), 1915–1927.

Xu, Q., & Chen, L. (1994). Characterization of cellulose film prepared from zinc-cellulose complexes. *Biomass and Bioenergy*, *6*(5), 415–417.

Zhu, S., Wu, Y., Chen, Q., Yu, Z., Wang, C., Jin, S., et al. (2006). Dissolution of cellulose with ionic liquids and its application: a mini-review. *Green Chemistry*, *8*(4), 325–327.